

EEE313 Term Project: Active Noise Canceling Headphones

Mustafa Mert Çetin 22003953, Samet Senai Işık 21901701

I. INTRODUCTION

Active noise cancelling (ANC) is a technology that is used to reduce or eliminate unwanted background noise in a variety of settings. It works by using microphones to detect ambient noise and generating an opposing sound wave, known as an "anti-noise," to cancel out the unwanted noise. ANC has been widely used in headphones and earbuds, allowing users to listen to music or make phone calls in noisy environments without being disturbed by background noise. It has also been applied in other areas, such as in aircraft cabins and office spaces, to create a more peaceful and productive environment. Despite its many benefits, ANC technology is not without its limitations.

In this project, we attempted to design and build a complete analog active noise cancelling (ANC) system for headphones. This approach is unusual in the industry, where digital designs are more commonly used, with analog components only used for environmental noise input and speaker outputs. We chose to pursue an analog solution due to the potential advantages of lower cost, lower distortion, and a more natural sound quality. We developed a working theory and tested it using MATLAB, and we also designed and built the necessary circuit blocks. Unfortunately, we were unable to fully complete the project due to time constraints. However, we present our work as a complete analog audio system consisting of an electret microphone, a microphone driver, a microphone amplifier, a phase shifter, a precise amplifier, and a speaker driver. Our total design provides a gain of approximately 420 and minimal distortion across all audible frequencies.

II. THEORY AND SOFTWARE IMPLEMENTATION

We have an electret microphone capsule for the noise input. Then we have a small circuit to drive microphone, shown in Fig. 1. The electret microphone needs a DC bias to operate, so we have connected it to the common voltage source of the system, $V_{dd} = 12\text{ V}$. We set the DC operating point to the middle, 6 V , so the resistor is chosen as same to the output impedance of the electret microphone capsule, which is $2.2\text{ k}\Omega$, and the next module is connected by a high-valued capacitor to DC isolate the modules.

Then we have the amplifier module. It consists of three stages, which are separated by again DC isolating capacitors, shown in Fig. 2. The input impedance seen from the base of the transistors, for the second and third stages, must be much higher than the DC biasing resistors to make the stage independent of the β of the transistors and prevent distortion. Also the DC biasing resistors must be much higher than the

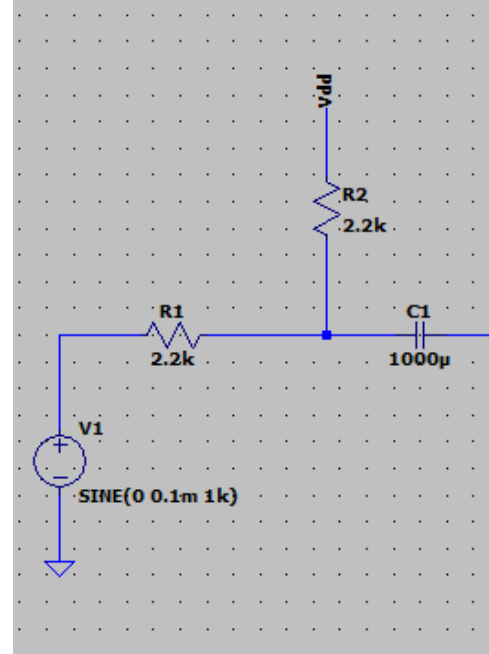


Fig. 1. Design of the microphone module in LTSpice.

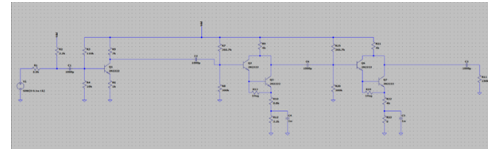


Fig. 2. Design of the all three stages of the amplifier module, in LTSpice.

previous stage's output impedance to prevent the load effect, and the resulting decrease in gain. Thus Darlington pairs are utilised to allow the DC biasing resistors to go much higher than they could otherwise. It also has a resistor ladder for the emitter resistors in the second and third stages to make the gain adjustable. The all three stages are shown in Fig. 3-5.

Next we have a phase shift module. But before that we need to have a buffer since the input impedance of the phase shift cannot be increased to desired levels, so that the effective input impedance seen by the previous amplifier module is high enough. We used LM324 ICs from Texas Instruments. But since they are not suitable for the higher audible frequency ranges, they distort the output if it changes polarity, i.e. goes from positive to negative or negative to positive, when the input exceeds a high enough frequency. Hence we needed to prevent output from changing polarity, and thus, we have DC

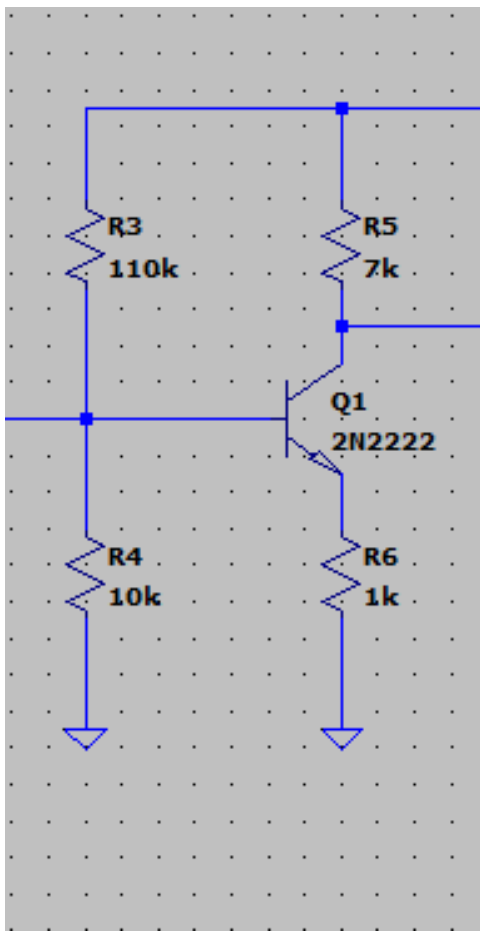


Fig. 3. Design of the first stage of the amplifier module, in LTSpice.

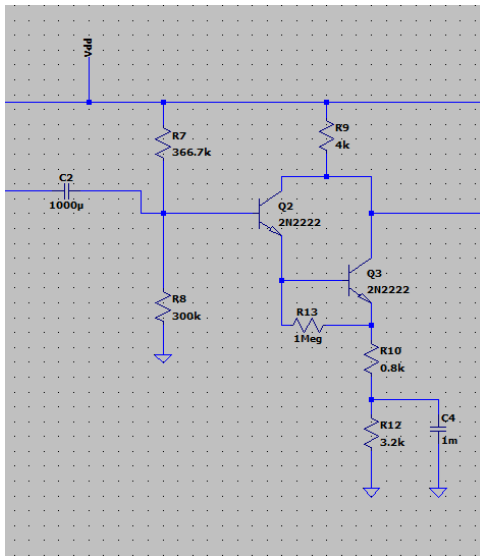


Fig. 4. Design of the second stage of the amplifier module, in LTSpice.

biased all the OPAMPs in the circuit, including the buffer, shown in Fig. 6.

Then we have the phase shift module, shown in Fig. 7. It is an All-Pass filter, that has the same gain for all the frequencies but different phase shifts for different frequencies.

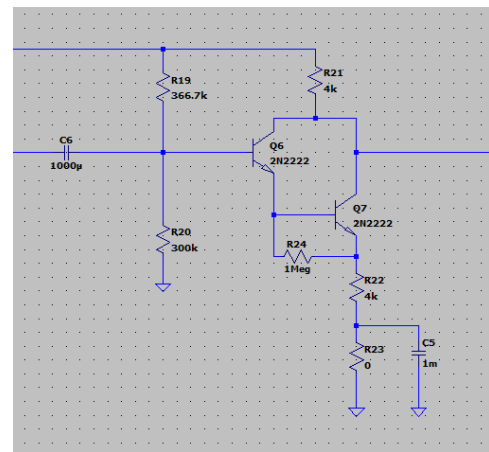


Fig. 5. Design of the third stage of the amplifier module, in LTSpice.

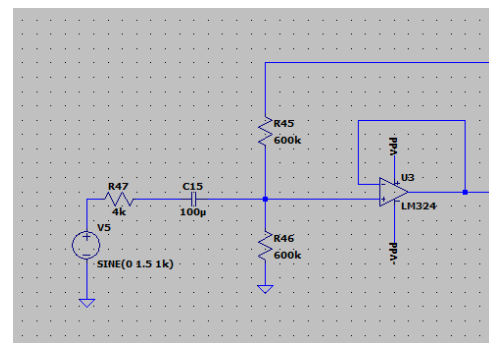


Fig. 6. Design of the DC biased buffer, in LTSpice.

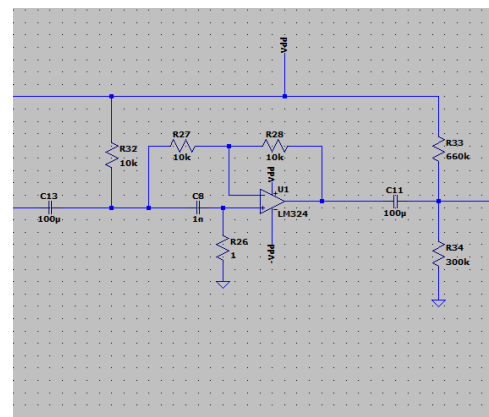


Fig. 7. Design of the phase shifter, in LTSpice.

The design and transfer function of an all-pass filter are shown in Fig. 8-9, respectively. Resulting gain and phase shift of the frequency response are also shown in Fig. 10. We have a variable capacitor to make the phase shift adjustable, and the OPAMP is DC biased to prevent the distortion issue explained earlier.

Then we have another amplifier built with an OPAMP, shown in Fig. 12. The formula for the gain is shown in Fig. 13. We have a trimpot used as R_f to make the gain adjustable. The purpose of this module is a precise adjustment to the gain. The earlier amplifier's resistor ladder allows a course adjustment,

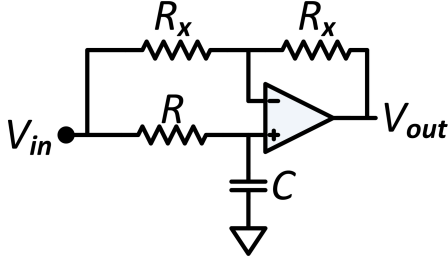


Fig. 8. Design of an all-pass filter.

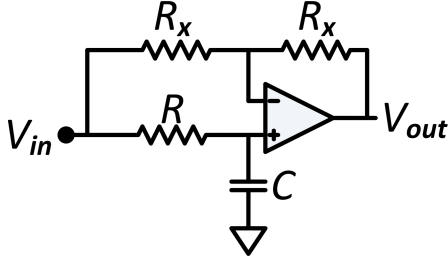


Fig. 9. Design of an all-pass filter.

$$H(s) = -\frac{s - \frac{1}{RC}}{s + \frac{1}{RC}} = \frac{1 - sRC}{1 + sRC},$$

Fig. 10. Transfer function of an all-pass filter.

$$|H(i\omega)| = 1 \quad \text{and} \quad \angle H(i\omega) = -2 \arctan(\omega RC).$$

Fig. 11. Gain and phase shift of an all-pass filter.

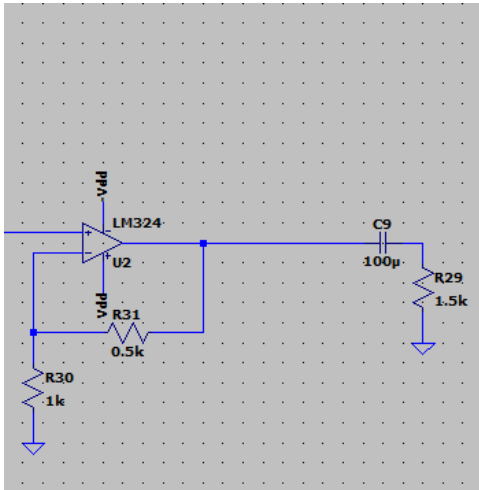


Fig. 12. Design of the precise amplifier, in LTSpice.

but this amplifier allows a precise adjustment thanks to the trimpot.

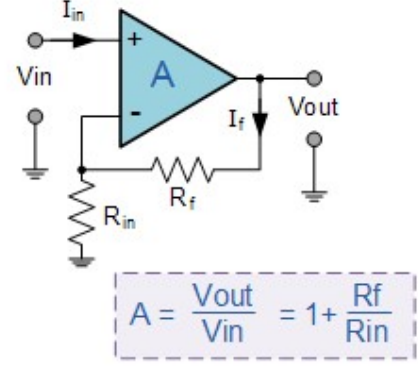


Fig. 13. Design and gain of a non-inverting OPAMP amplifier.

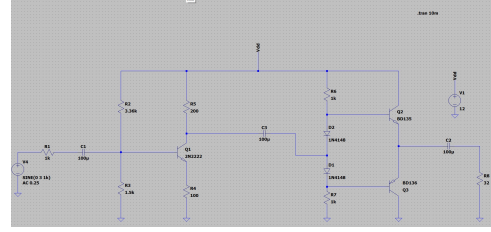


Fig. 14. Design of the driver module, in LTSpice.

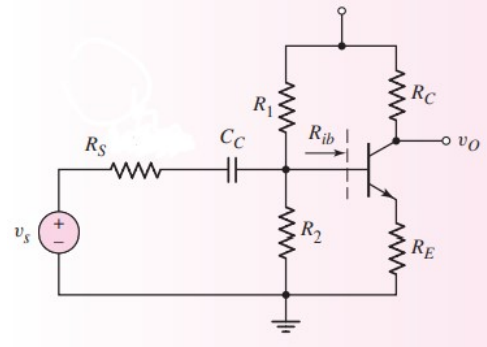


Fig. 15. Generic design of a Class A amplifier.

Then lastly we have our driver module. It is a two-stage amplifier consisting of class A and class AB amplifier cascaded together, as shown in Fig. 14. The general design of a Class A amplifier is shown in Fig. 15. Its AC equivalent circuit and the formula for the gain are shown in Fig. 16-17, respectively.

The first stage has a gain of approximately -0.7, and the second stage has a gain of approximately unity, and thus, overall gain is about -0.7, as shown in Fig. 18.

III. HARDWARE IMPLEMENTATION

We have built each module on breadboards. The overall circuit, and modules separately are shown in Fig. 19-25.

IV. RESULTS

We have tested the quality of the system by playing a music to the microphone and listening to the headphones. The audio

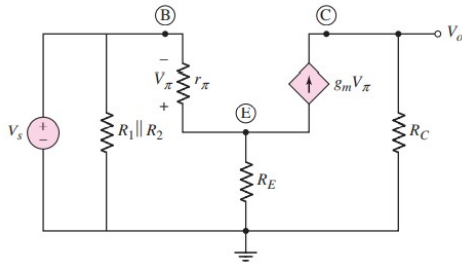


Fig. 16. AC equivalent circuit of a Class A amplifier.

$$A_v = \frac{-\beta R_C}{r_\pi + (1 + \beta) R_E} \left(\frac{R_i}{R_i + R_S} \right)$$

Fig. 17. The formula for gain of a Class A amplifier.

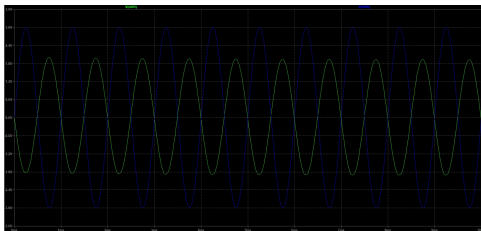


Fig. 18. The graph of input and output for the driver module, with an input V_{pp} of 6 V, in LTSpice.

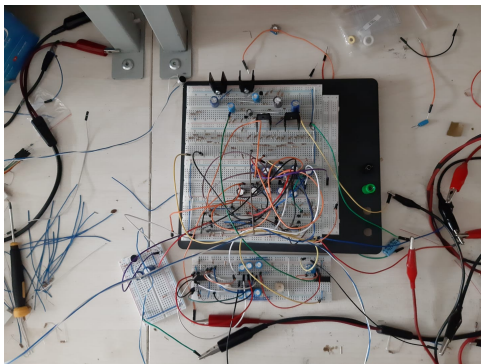


Fig. 19. The overall circuit.

recording of the headphone output, and the corresponding video recording on an oscilloscope can be seen [here](#) and [here](#).

We have played a sine wave from a speaker, using a signal generator. The frequency of the sine wave was 1 kHz. We had a microphone listen to the speaker, in a setup shown in Fig. 26. The voltage levels measured at different points of the circuits are shown in Fig. 27-29.

We have also examined the frequency components of the output, when the input is a sine wave and a square wave. The corresponding frequency components can be seen in Fig. 30-31, respectively. The output for the sine wave is mostly clean of harmonic byproducts, whereas square wave contains a great number of harmonic components.

We have also given a 10 mV peak-to-peak sine wave for

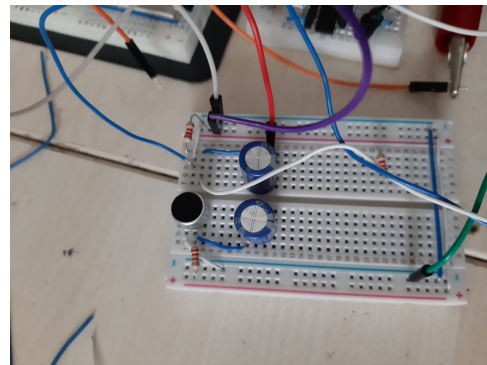


Fig. 20. The microphone module.

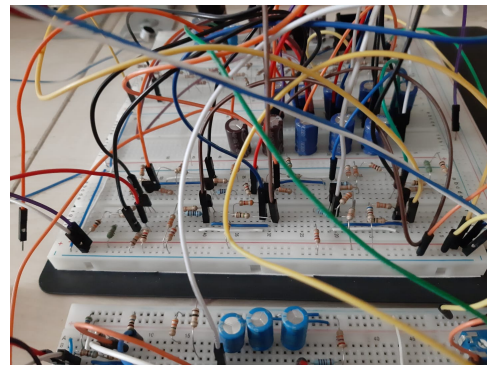


Fig. 21. The microphone amplifier.

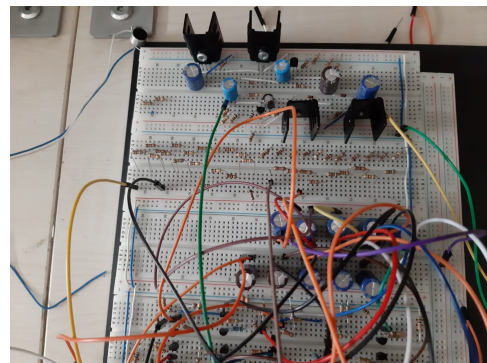


Fig. 22. The resistor ladder for the microphone amplifier, for a coarse adjustment in gain.

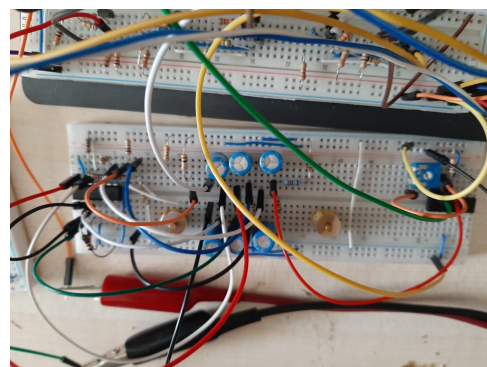


Fig. 23. The buffer, phase shift and the precise amplifier modules together.

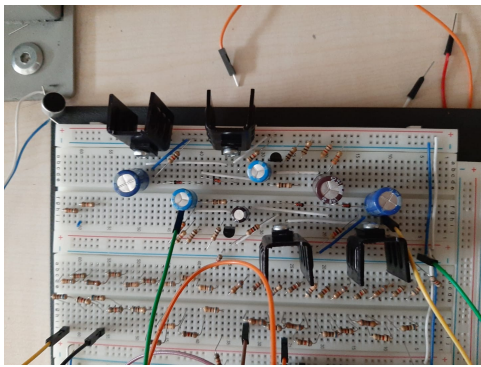


Fig. 24. The speaker driver.

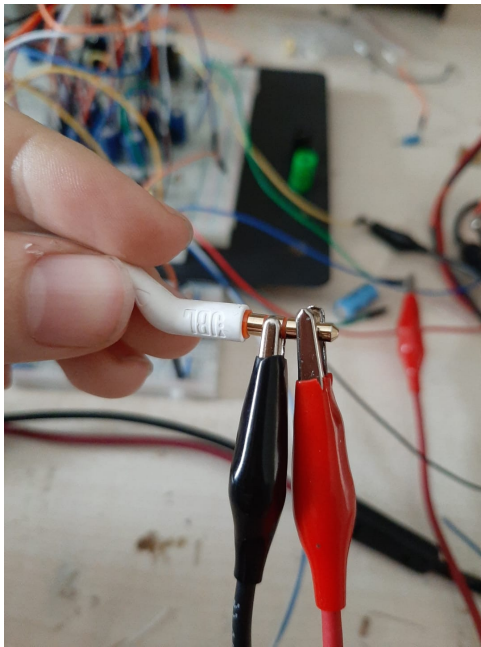


Fig. 25. The connection to the headphones.

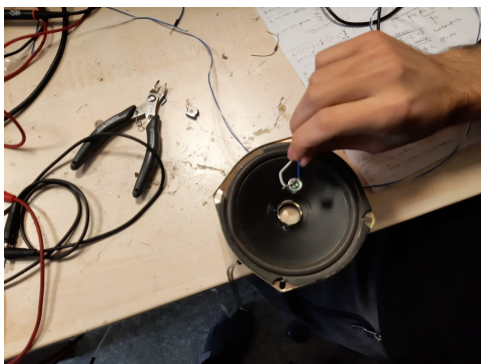


Fig. 26. The setup to measure the voltages at various points due to the sine wave given by the speaker.

the place of the microphone output to examine the frequency characteristics of the circuit. The maximum gain occurs at a range about 1 kHz and is about 236. The cutoff frequencies are 17 Hz and 230 kHz. The related measurements are given in Fig. 31-33.

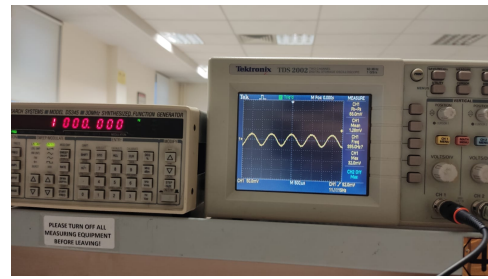


Fig. 27. The output of the microphone module.

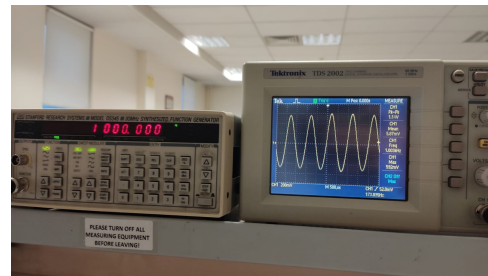


Fig. 28. The output of the microphone amplifier

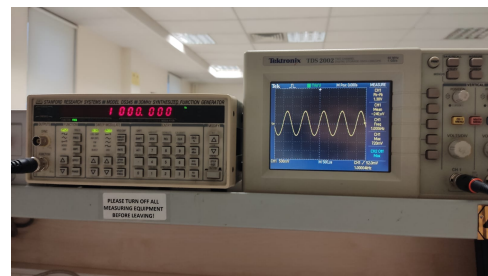


Fig. 29. The overall output.

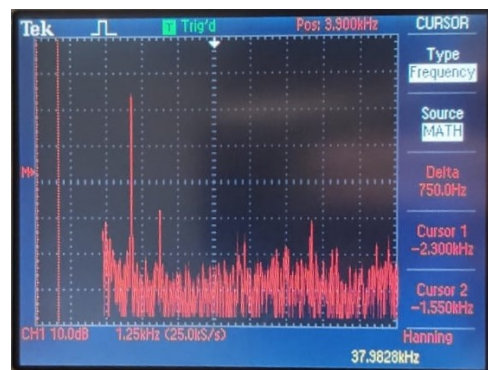


Fig. 30. The frequency components of the sine wave.

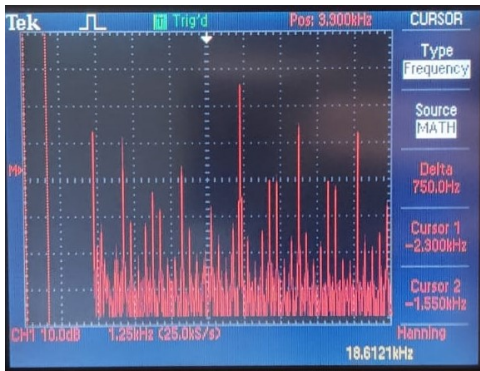


Fig. 31. The frequency components of the square wave.

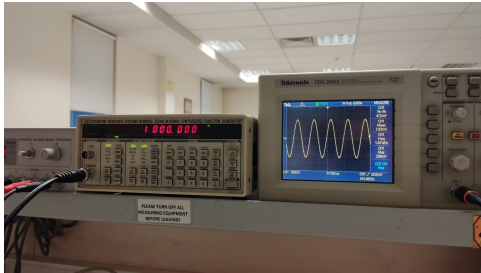


Fig. 32. The maximum gain.

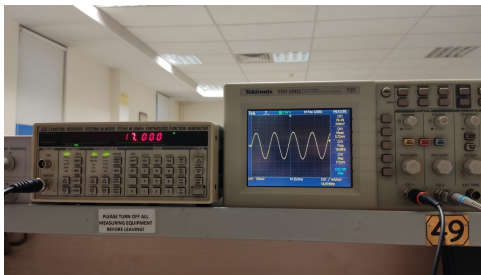


Fig. 33. The lower cut-off point.

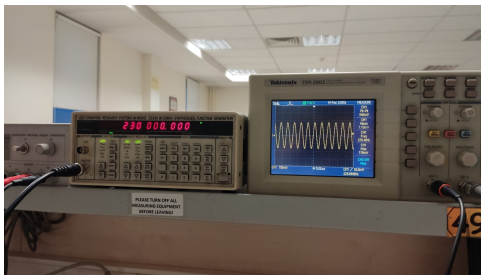


Fig. 34. The higher cut-off point.

V. CONCLUSION

The circuit modules worked as intended, and the system successfully works as an analog audio system with variable gain and phase shift. We have achieved the gain and phase shift properties that we have desired in the real circuit implementation without any unaccounted-for problems. So in a sense, we have completed the initial steps to a total ANC system. We might consider to pursue our initial ANC idea in the future as a continuation project, using our circuit blocks we have designed and built here.